REVIEW ARTICLE

Role of ultrasound in the treatment of pediatric infectious diseases: case series and narrative review

Takahiro Hosokawa[1] · Yutaka Tanami[1] · Yumiko Sato[1] · Kuntaro Deguchi[2] · Haruka Takei[2] · Eiji Oguma[1]

Abstract

Background Infectious diseases are common in pediatric patients. In these patients, ultrasound is a useful imaging modality that involves no irradiation or sedation and can be performed repeatedly at the patient's bedside. The purpose of this review was to show pediatric cases with infectious disease that used ultrasound to decide the methods of treatment.

Data sources Literature review was performed using Pubmed as the medical database source. No year-of-publication restriction was placed. The mesh terms used were: "ultrasound", "sonography", "infectious disease", "treatment", "antibiotics", "surgical intervention", "pediatric", "children", "deep neck abscess", "pyothorax", "empyema", "pneumonia", "urinary tract infection", "intra-abdominal abscess", "soft tissue infection", "septic arthritis", "osteomyelitis", and "surgical site infection".

Results We presented pediatric case series with infectious diseases, including deep neck abscess, pyothorax and empyema, pneumonia, urinary tract infection, intra-abdominal abscess, soft tissue infection, septic arthritis and osteomyelitis, and surgical-site infection. Ultrasound was useful for evaluating the extent and location of inflammation and abscess and for decision-making concerning surgical intervention.

Conclusion Knowledge of these sonographic findings is important for sonographers during examinations and for physicians when determining the treatment plan and period of antibiotic therapy for infected lesions.

Introduction

Infectious diseases are common in pediatric patients [1–5]. Medical history, physical examination, and laboratory studies are always needed to diagnose infectious diseases [2, 6, 7]. In addition, imaging examinations, such as radiography, ultrasound, computed tomography (CT), and magnetic resonance imaging (MRI), are useful for the diagnosis and evaluation of infectious diseases.

In pediatric patients, unlike other imaging modalities, ultrasound is a useful modality because it involves no irradiation or sedation and can be performed repeatedly at the patient's bedside [6, 8]. In addition, pediatric patients sometimes present with nonspecific clinical signs; therefore, ultrasound is useful to evaluate directly various locations suspected of being affected by an infectious disease [9].

To our knowledge, there are only a few reports focus on ultrasound to determine the treatment plan for pediatric infectious diseases [10]. The purposes of this review were to provide basic knowledge of pediatric infectious diseases occurring in various locations and to describe the sonographic imaging findings for decision-making regarding treatment and period of antibiotic therapy.

Case series and data sources of the literature review

Case series

We presented pediatric case series with infectious diseases, including deep neck abscess, pyothorax and empyema, pneumonia, urinary tract infection, intra-abdominal abscess, soft tissue infection, septic arthritis and osteomyelitis, and surgical-site infection.

✉ Takahiro Hosokawa
snowglobe@infoseek.jp

1 Department of Radiology, Saitama Children's Medical Center, 1-2 Shintoshin Chuo-ku, Saitama 330-8777, Japan

2 Department of Infectious Diseases and Immunology, Saitama Children's Medical Center, Saitama, Japan

Ultrasound

Recently, portable ultrasound machines of varying sizes, as opposed to traditional full-platform machines, are used at the patient's bedside. This system is known as the point-of-care ultrasound and has been widely embraced in various situations, such as emergency medicine. However, in this case series, the sonographic examination was performed by one of four pediatric radiologists (with 25, 20, 15, and 12 years of clinical experience, respectively, in pediatric ultrasonography) using a 5–15 MHz convex or linear transducer (LOGIQ 7, E9, S8, and E10; GE Healthcare, Waukesha, WI) with traditional full-platform machines. If pediatric patients were located in the emergency room or intensive care unit, traditional full-platform machines were used at the patient's bedside.

Data sources

Literature review was performed using Pubmed as the medical database source. No year-of-publication restriction was placed. The mesh terms used were: "ultrasound", "sonography", "infectious disease", "treatment", "antibiotics", "surgical intervention", "pediatric", "children", "deep neck abscess", "pyothorax", "empyema", "pneumonia", "urinary tract infection", "intra-abdominal abscess", "soft tissue infection", "septic arthritis", "osteomyelitis", and "surgical site infection".

Deep neck infection

Background

Deep neck infection occurs in the potential cavity or spaces between the layers of the deep cervical fascia and may result in life-threatening complications, such as compression of the airway, mediastinitis, thrombosis of the internal jugular vein, or septic shock [11, 12]. This infection includes peri-tonsillar (Fig. 1a, b), parapharyngeal, and retropharyngeal (Fig. 1c–e) abscess, and infection of these locations may extend to prevertebral, submandibular, or danger space abscess [11, 12]. These abscesses are caused by an upper aero-digestive tract infection, odontogenic infection, or direct invasion from adjacent tissue infections [11–13]. The retropharyngeal space is divided into the right and left sides, and a lymph node communicates with the nasopharynx area in this space. This communication disappears by puberty; therefore, retropharyngeal abscesses tend to occur in young children [14].

Method of ultrasound

Among cervical infectious diseases, tonsillitis and peri-tonsillar abscesses, which are common in pediatric patients, can be detected by ultrasound imaging [15, 16]. Cervical ultrasound is usually performed in pediatric patients in the supine position. A neck axial sonogram is obtained from the patient's mandible to the thoracic inlet. The thyroid, salivary glands, and trachea are also evaluated [17, 18]. The tonsil is evaluated using the submandibular approach. Probes held underneath the mandible and tonsil are visualized via the submandibular gland [16, 19].

Discussion of the interpretation of the sonographic findings of deep neck abscess

Surgical intervention and approach route are decided based on the clinical symptoms and the location, size, and cause of the abscess. However, when there is a symptom-associated airway compression, urgent intervention is needed [12, 20]. In deep neck abscesses, information regarding the abscess size is useful to recommend surgical intervention, and its location is necessary to decide the surgical approach route. The longest diameter of approximately 2 cm was reported to be valuable in recommending surgical intervention [12, 20, 21].

Pyothorax/empyema

Background

Pyothorax and empyema are divided into the following three stages: simple exudative stage, when there is clear fluid accumulation with a low white cell count within the pleural cavity (simple/uncomplicated parapneumonic effusion); fibrinopurulent stage (Fig. 2a, b), when septation and loculations occur, with an increase in white cells within the pleural cavity resulting in pus (complicated parapneumonic effusion), which eventually becomes overt pus (empyema); and the final organizing stage (Fig. 2c, d), when there are thick and non-elastic intra-pleural membranes (the peel) within the pleural cavity, which may prevent lung re-expansion (trapped lung) [3, 22, 23]. The stages of pyothorax and empyema are correlated with the span of inflammation within the thorax [23, 24]. Surgical intervention, such as drainage, and treatment period may be decided based on these stages [24].

Method of ultrasound

Visualization of the lung and pleural cavity between bones, such as the ribs or clavicle, known as the intercostal view, and the approach around the sternum, such as
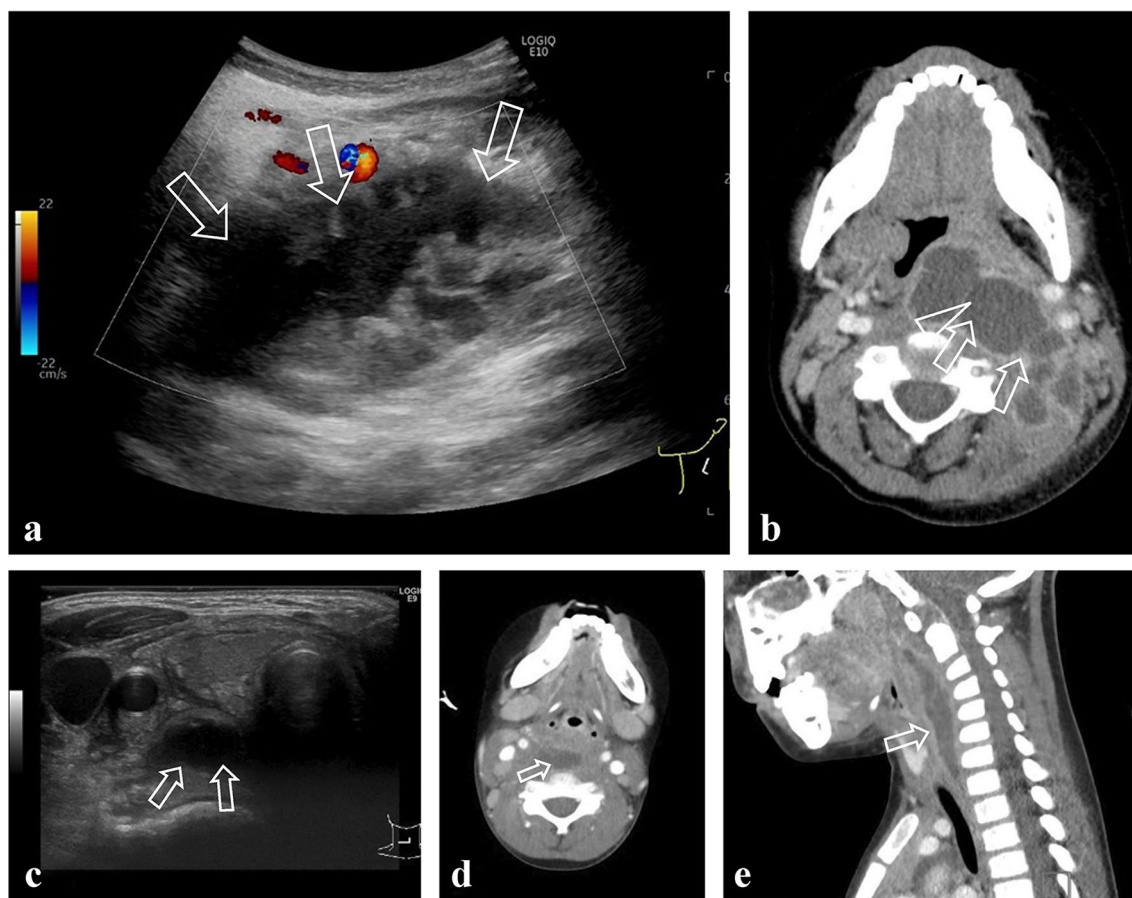
Fig. 1 a, b Imaging findings of a five-year-old male patient with peri-tonsillar abscess. Snoring was evident two days before. His temperature was 39.8 °C and oxygen saturation (SpO$_2$) was 97% (room air). Blood test results revealed a white blood cell count of 20,200/mm^3 and C-reactive protein of 9.26 mg/dL. Ultrasound and computed tomography (CT) revealed an abscess around the tonsil. CT revealed compression of the trachea to the right side. The transverse diameter of the abscess was 5 cm, which exceeds 2 cm; thus, surgical intervention for drainage was performed based on the size of the abscess. Bacteriological examination revealed *Streptococcus pyogenes* in the pus. Intravenous antibiotics therapy was performed for four weeks and subsequently switched to oral antibiotic therapy. The treatment was considered successful. **a** Oblique color Doppler sonogram showing a peri-tonsillar abscess (arrows). Low-echoic fluid collection surrounds the rippling wall; hence, abscess formation was diagnosed. **b** Axial contrast-enhanced CT showing the compression of the trachea to the right side (arrowhead). The transverse diameter of the abscess was 5 cm (arrows). Surgical intervention for drainage was performed based on the size of the abscess. **c–e** Imaging findings of a three-year-old male patient with retropharyngeal abscess. He had cervical pain one week before. His temperature was 38.9 °C, and oxygen saturation (SpO$_2$) was 99% (room air). Blood test results revealed a white blood cell count of 20,300/mm^3 and C-reactive protein of 10.9 mg/dL. Ultrasound revealed fluid collection behind the thyroid; however, the inferior side was not clearly evaluated, and CT was recommended. CT revealed that the lesion was limited to the retropharyngeal space. Abscess drainage was performed for the identification of the bacteria and to prevent the progression of mediastinitis. *Streptococcus pyogenes* was detected in the pus. Intravenous antibiotic therapy was performed for two weeks and subsequently switched to oral antibiotic therapy. The treatment was considered successful. **c** Transverse sonogram showing fluid collection behind the thyroid, which was diagnosed as a retropharyngeal abscess (arrows). **d** Axial contrast-enhanced CT showing the retropharyngeal space (arrow). **e** Sagittal contrast-enhanced CT showing the retropharyngeal space (arrow). This lesion did not extend to the mediastinum

the parasternal, trans-sternal, and sub-xiphoid views, are useful for evaluating pyothorax and empyema [25, 26]. The posterior para-spinal approach also may be useful. Change in the patient's position may be required for accurate evaluation of pleural effusion.

Discussion of the interpretation of the sonographic findings of pyothorax/empyema

Ultrasound can evaluate pleural effusion, and the findings are classified based on the above-mentioned three stages

Fig. 2 a, **b** Imaging findings of an eight-year-old male patient with pyothorax/empyema with fibrinopurulent pleural effusion. He had a cough and high fever one month before. He also had swelling and a reddish rash on the right side of his chest. His temperature was 38.0 °C, and oxygen saturation (SpO$_2$) was 94% (room air). Blood test results revealed a white blood cell count of 18,600/mm^3 and C-reactive protein of 13.4 mg/dL. Coronal reconstructed contrast-enhanced computed tomography (CT) revealed a massive pleural effusion in the right thorax. Ultrasound revealed a huge complex pleural effusion with multiple septation, and pyothorax/empyema with fibrinopurulent pleural effusion was diagnosed. Surgical drainage was performed. *Streptococcus intermedius* was detected, and intravenous antibiotics therapy was administered for two months. The treatment was considered successful. **a** Transverse sonogram showing a huge complex pleural effusion with multiple septations (arrows). **b** Coronal reconstructed contrast-enhanced CT showing a massive pleural effusion (arrows) and atelectasis (arrowhead). The internal septa within the pleural effusion could not be visualized. **c**, **d** Imaging findings of a 11-year-old male patient with pyothorax/empyema with organizing pleural effusion. He had a high fever 20 days before, and pleural effusion was detected on the chest radiograph. A chest drain tube was introduced; however, efficient aspiration could not be performed. Sagittal reconstructed contrast-enhanced CT revealed pleural effusion and atelectasis. Sagittal sonogram revealed pleural effusion with echogenic components, multiple small septations, and thickened pleura. Pyothorax/empyema with organizing pleural effusion was diagnosed. Based on the sonographic findings, space for aspiration of the collected fluid by the drainage tube was absent. Therefore, the drainage tube was removed, and antibiotic therapy was continued; further surgical intervention was not performed. Finally, pleural effusion decreased. **c** Sagittal sonogram showing pleural effusion with echogenic components and multiple small septations (arrow). A thickened pleura and atelectasis without air infiltration are also seen (arrowheads). Fluid collection for aspiration by the drainage tube was absent. **d** Sagittal reconstructed contrast-enhanced CT showing pleural effusion (arrows) and atelectasis (arrowheads)

[23, 27]. Free-flowing effusion corresponds to simple exudative pleural effusion, septations or loculations correspond to fibrinopurulent pleural effusion, and visceral pleural thickening with trapped lung corresponds to organizing pleural effusion [23]. Real-time lung ultrasound may evaluate lung motion and may determine the presence or absence of trapped lungs [27].

Pneumonia

Background

Pneumonia is one of the causes of death and long hospitalization in pediatric patients. Physical evaluation, laboratory data, and chest radiography are used to diagnose pneumonia.
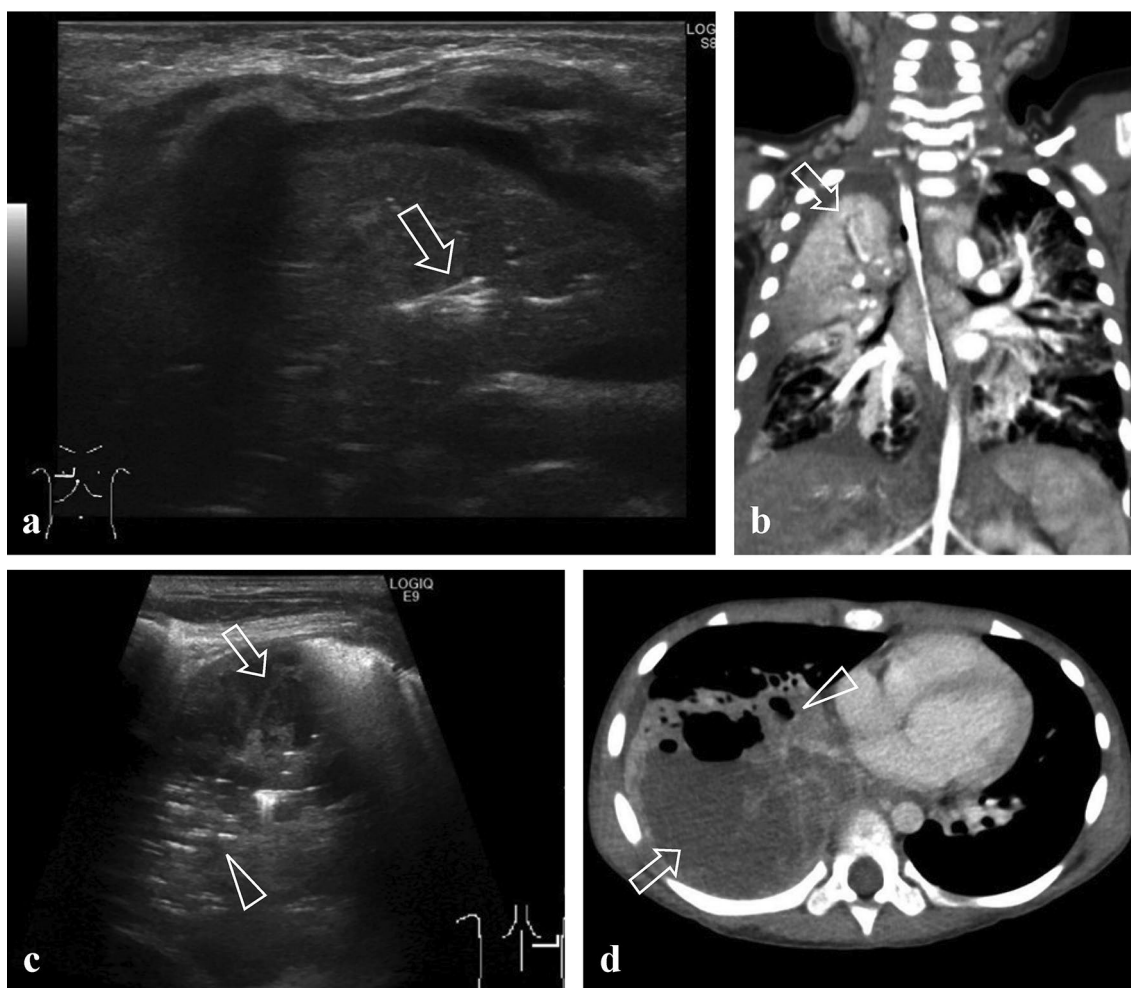
Fig. 3 a, **b** Imaging findings of a 11-month-old female patient with pneumonia. She had a high fever 14 days before, and consolidation was detected on the chest radiograph. Her temperature was 40.0 °C, and oxygen saturation (SpO_2) was 90% (room air). Blood test results revealed a white blood cell count of 22,400/mm^3 and C-reactive protein of 40.0 mg/dL. Ultrasound and coronal reconstructed contrast-enhanced computed tomography (CT) revealed consolidation in the right upper lobe. Pneumonia was diagnosed. Antibiotic therapy was continued for three weeks and the treatment was considered successful. **a** An ultrasound image from the right anterior upper lung zone shows air bronchograms represented by punctate hyperechoic specks within the lesion (arrow). **b** Coronal reconstructed CT shows a focal dense opacification in the right upper lobe (arrow). There are additional areas of consolidation in the right and left lower lobes.

c, **d** Imaging findings of a four-year-old female patient with a lung abscess. She had a second incidence of pneumonia. She had a high fever before one month. Her temperature was 38.8 °C, and oxygen saturation (SpO_2) was 92% (room air). Blood test results revealed a white blood cell count of 24,410/mm^3 and C-reactive protein of 3.14 mg/dL. Ultrasound and constructed contrast-enhanced CT revealed a huge lung abscess. Antibiotic therapy was continued for three weeks; further surgical resection was performed for the residual lung cystic area. **c** Lung ultrasound of the right lower lobe showing a well-circumscribed, hypoechoic lung abscess (arrow) within the consolidated lung (arrowhead). The longest diameter was 5 cm. **d** Contrast enhanced CT shows a large cavitary lesion in the right lower lobe (arrow). Consolidation is detected in anterior lesion (arrowhead). The lesion size was 6×5 cm

Recently, ultrasound has been used to diagnose pneumonia and to monitor the response to treatment (Fig. 3a, b) [28, 29]. Treatment plan varies according to the pathogen that caused pneumonia, the type of pneumonia (such as community acquired pneumonia or aspiration pneumonia in hospitalized children), patient's age, underlying diseases, and presence or absence of lung abscesses (Fig. 3c, d) [30–35]. Effectiveness of antibiotic treatment can be evaluated based on the clinical findings and image findings. Lung ultrasound was reported to be useful to monitor treatment effect and to evaluate the size of consolidation and abscess [28, 36, 37]. Surgical procedures for drainage or pulmonary resection may be required in cases that do not respond adequately to antibiotic treatment [37, 38]. In addition, lung ultrasound was reported to be useful to diagnose and predict the severity of acute bronchiolitis [39–41].
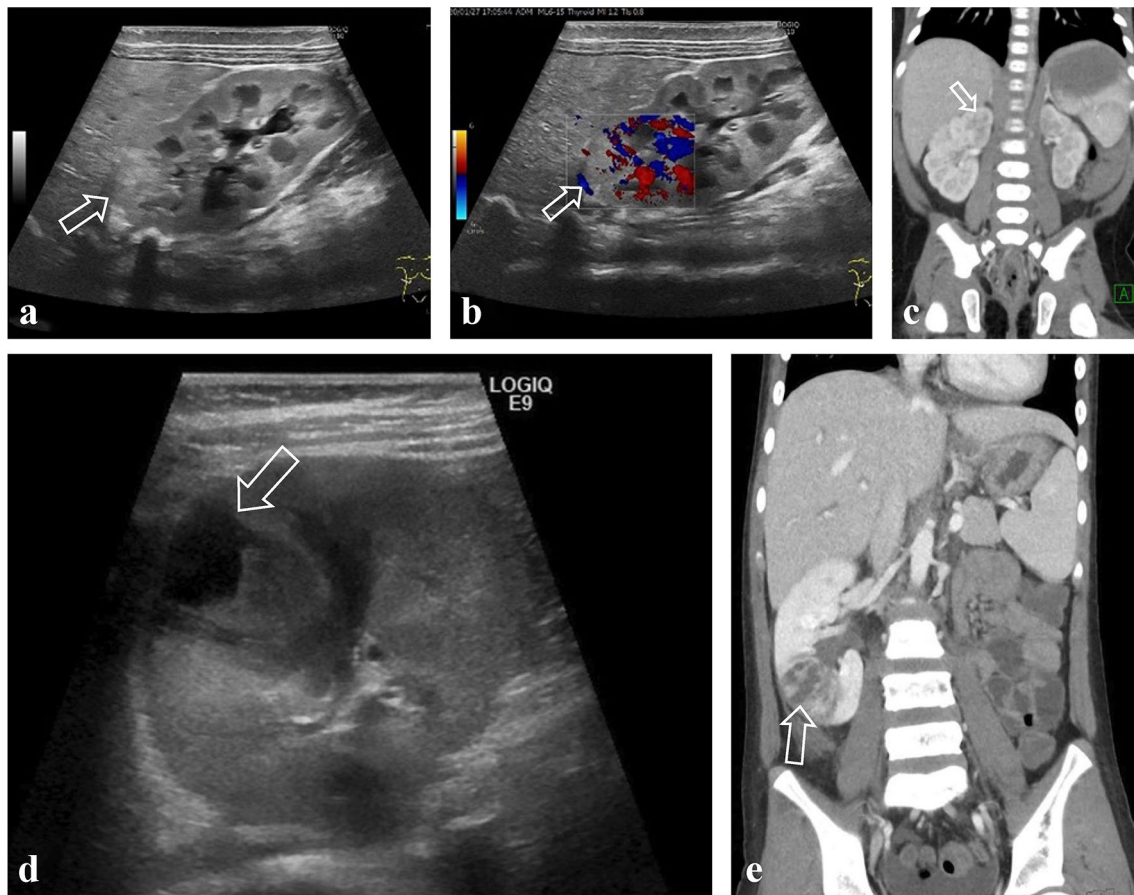
Fig. 4 **a–c** Imaging findings of a four-month-old male patient with acute focal bacterial nephritis (AFBN). He had a third urinary tract infection. His temperature was 38.0 °C. Blood test results revealed a white blood cell count of 27,500/mm^3 and C-reactive protein of 9.7 mg/dL. Ultrasound demonstrated a focal area of loss of cortico-medullary differentiation and hyper-echogenicity with decreased enhancement compared with other areas on the coronal reconstructed computed tomography (CT). AFBN was diagnosed. An adequate treatment period of three weeks, and not two weeks as for acute pyelonephritis, was conducted for AFBN. **a** Oblique sonogram demonstrating a focal area of loss of cortico-medullary differentiation and hyper-echogenicity (arrow). **b** Oblique color Doppler sonogram showing diminished flow in the area of cortico-medullary differentiation and hyper-echogenicity (arrow). **c** Coronal reconstructed CT showing right renal enlargement. The upper pole of the right kidney shows decreased enhancement compared with other areas (arrow). AFBN was diagnosed. **d**, **e** Imaging findings of a 10-year-old male patient with renal abscess. He had back pain three days before and a high fever. His temperature was 39.5 °C. Blood test results revealed a white blood cell count of 7800/mm^3 and C-reactive protein of 21.4 mg/dL. Blood and urine cultures were positive for *Escherichia coli*. Ultrasound and CT revealed a hypoechoic or a low-attenuation mass in the right kidney. The patient was diagnosed with a renal abscess. The longest diameter did not exceed 3 cm; therefore, antibiotic therapy without surgical intervention was performed. The treatment was considered successful. **d** Axial sonogram showing a hypoechoic mass with loss of cortico-medullary differentiation and a hypoechoic area in the right kidney (arrow). **e** Coronal reconstructed CT showing a low-attenuation mass in the right kidney (arrow). The patient was diagnosed with a renal abscess. The longest diameter was not greater than 3 cm

Methods of ultrasound

To evaluate the lung, a structured systematic approach was recommended first [28, 29]. However, a focused approach was also useful for evaluating regions that were already detected by other modalities, such as chest radiograph or computed tomography. A previous study reported a systematic approach in which the lung was divided into anterior, lateral and posterior zones, and then subdivided into upper and lower halves using parasternal, mid-clavicular, anterior axillary, mid-axillary, posterior axillary, mid-scapular, and paravertebral approach [42]. As a limitation of lung ultrasound, the region located deep from the pleura accompanying with located air-filled lung
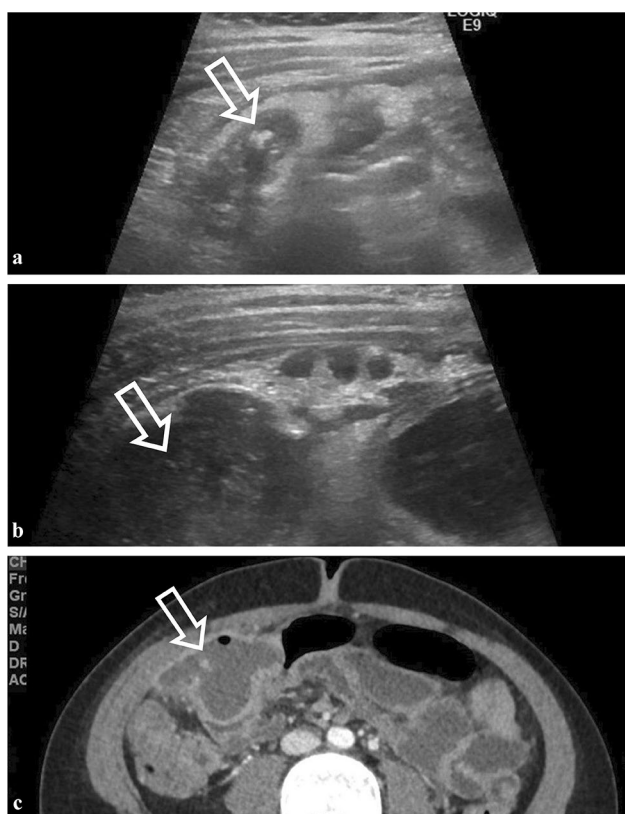
Fig. 5 Imaging findings of a five-year-old male patient with intra-abdominal abscess caused by appendicitis. **a** Transverse sonogram showing the dilated appendix and hyper-echogenicity around the appendix. **b** Abscess formation is revealed by hyper-echogenicity. **c** Low attenuation with a thickened wall is seen. Air bubbles were detected within the abscess. The patient was diagnosed with appendicitis with abscess formation

parenchyma between the pleura and the region was not visualized.

Discussion of the interpretation of the sonographic finding of pneumonia

Although an air-filled lung parenchyma could be directly visualized using ultrasound, the following two characteristic artifactual lines have been mentioned: A-lines hyperechoic lines running parallel to the pleural line as reverberation artifacts of the pleural line, and B-lines as comet-tail artifacts: hyperechoic lines arising from the pleura toward to the hilar area. The following sonographic findings of pneumonia as consolidation due to

fluid collection within alveolar area have been reported: the absence of A-lines within the area; increased B-lines surrounding the area of consolidation and arising from the deep edge of the consolidation, and presence of sonographic air bronchograms [28, 29, 35, 42]. Lung abscess may be detected as a low echoic area within the consolidation [36]. Severity of bronchiolitis corresponds to the degree of coalescence of B-lines on lung ultrasound. Compared to the cases with non-coalescence of B-lines, the cases with coalescence of B-lines or sub-pulmonary consolidation needed more intensive treatment [39–41, 43–46]. Lung ultrasound was also reportedly useful in monitoring the treatment effect for evaluating the size of the consolidation and the abscess [28, 36, 37]. Surgical procedures for drainage or pulmonary resection may be required in cases that do not respond adequately to antibiotic treatment [37, 38]. In addition, in cases of COVID-19 lung ultrasound was useful to demonstrate lung interstitial changes, consolidation, and pleural effusion [45, 47, 48].

Urinary tract infection

Background

Pediatric urinary tract infections are a common problem, and febrile urinary tract infection usually manifests as acute pyelonephritis (APN), acute focal bacterial nephritis (AFBN), which is also known as acute lobar nephronia, or renal abscess [49, 50]. The differentiation of APN, AFBN (Fig. 4a–c), and renal abscess (Fig. 4d, e) during the acute phase is important because the recommended treatment durations and necessity of surgical intervention differ in these conditions [51]. A three-week course of intravenous and oral antibiotic therapy, rather than a two-week course, is recommended for pediatric patients with AFBN [51]. Cases of large abscesses, such as those larger than 3 cm, might require surgical intervention [52, 53].

Methods of ultrasound

The kidney is usually visualized in the supine position or left or right lateral decubitus position. The prone position is also useful for evaluating the kidneys. The urethra is visualized using a water-filled bladder as an acoustic window. The perineal approach is also useful for evaluating the urethra [54, 55].
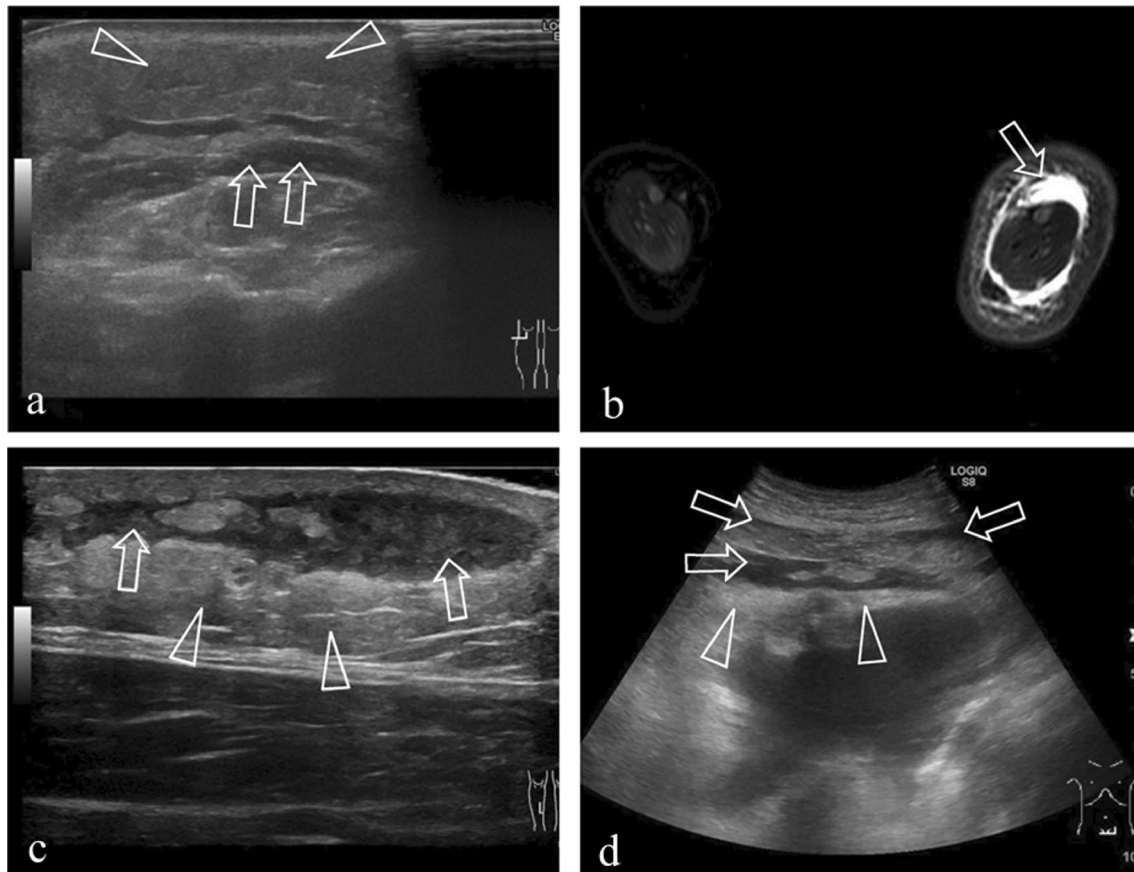
Fig. 6 **a**, **b** Imaging findings of a five-month-old female patient with severe cellulitis. She had a left leg swelling two days before. Her temperature was 38.0 °C. Blood test results revealed a white blood cell count of 27,600/mm^3 and C-reactive protein of 12.9 mg/dL. Ultrasound revealed fluid collection in the superficial fascia. Thickness of the fluid collection was greater than 2 mm; thus, necrotizing fasciitis was suspected. Therefore, magnetic resonance imaging (MRI) was recommended to evaluate the deep fascia. MRI revealed fluid on the superficial fascia but not around the deep fascia. Surgical decompression was performed for compartment syndrome. Inflammation did not extend to the fascia, and severe cellulitis was diagnosed. Blood culture revealed *Staphylococcus haemolyticus*. Therefore, intravenous antibiotic therapy was administered for two weeks resulting in successful treatment. **a** Fluid collection was visualized on the superficial fascia (arrows). High echogenicity within the subcutaneous tissue was observed (arrowheads). **b** Fat suppression T2-weighted axial MRI showing fluid on the superficial fascia and not around the deep fascia (arrows). Surgical intervention was performed, and severe cellulitis was diagnosed. **c** Ultrasound image of a 14-year-old female patient with cellulitis and abscess formation. She had experienced

leg swelling 10 days before. Her blood test results revealed a white blood cell count of 13,700/mm^3 and C-reactive protein of 2.2 mg/dL. Cellulitis and abscess formation were diagnosed by ultrasound, and surgical drainage was performed. Intravenous antibiotic therapy was administered for two weeks, and the treatment was considered successful. High echogenicity within the subcutaneous tissue was observed (arrowheads). Abscess formation was evident, and the diameter was 2×7 cm (arrows). Surgical drainage was performed. **d** Ultrasound image of a 12-year-old male patient with necrotizing fasciitis. He had a high fever and a swelling around the abdomen following bone marrow transplantation. He had septic shock, and the blood culture revealed *Pseudomonas aeruginosa*. Ultrasound showed fluid collection, with a thickness greater than 2 mm, around the rectus abdominis; therefore, necrotizing fasciitis was suspected. To decompress and achieve debridement, surgical intervention was performed, and necrotizing fasciitis was diagnosed. Fluid collection was detected around the rectus abdominis (arrows). High-echoic edema was also detected around the effusion (arrowheads). Thickness of the fluid collection was greater than 2 mm, therefore, necrotizing fasciitis was suspected

Discussion of the interpretation of the sonographic findings of urinary tract infection

In recent studies on treatment plan decisions, although AFBN diagnoses were based on imaging findings obtained using CT, ultrasound could detect AFBN [51, 56]. AFBN was reported to be the midpoint in the spectrum between APN and renal abscesses [49, 57]. Therefore, APN was diagnosed based on the presence of diffuse nephromegaly, while AFBN was diagnosed based on the presence of focal loss of cortico-medullary differentiation, and renal abscess was diagnosed as a low echoic area in the kidney by ultrasound [52, 56, 58, 59]. Focal hyper-echogenicity and swelling, with loss of cortico-medullary differentiation, may present as an acute phase of urinary tract infection. Focal atrophy may present as a chronic phase [56]. In cases of repeated urinary tract infection, congenital anomalies should be evaluated [5].

Intra-abdominal abscess

Background

Intra-abdominal abscesses are caused by various inflammatory diseases, including inflammatory bowel disease, appendicitis (Fig. 5a–c), and digestive tract perforation [60]. Management of intra-abdominal abscess, including surgical intervention, differs based on the etiology of the abscess [61–63]. Information regarding the presence or absence of the abscess and its location is important to decide the access route for the abscess and its management [60–62, 64].

Method of ultrasound

Ultrasound can evaluate the presence of an abscess and also determine its location, size, and access route [4, 65]. In addition, ultrasound can detect the cause of the abscess [4, 66].

Discussion of the interpretation of the sonographic findings of intra-abdominal abscess

Retroperitoneal or intramuscular abscesses can also be detected by ultrasound. However, in some cases, the ultrasound cannot sufficiently examine the abscess owing to a blind area behind the dilated intestine. In case of abdominal pain or distention, pediatric patients cannot stay in the same position for a long time. Hence, in some cases, a sufficient examination cannot be performed. In such cases, although sedation may be required, CT or MRI examination is recommended [67].

Soft tissue infection

Background

Soft tissue infection includes cellulitis, which involves the subcutaneous tissue only (Fig. 6a, b), and fasciitis, which involves the fascia [68]. Cellulitis is usually treated with antibiotics alone [68]. In cases of cellulitis with an abscess (Fig. 6c), incision and drainage may be needed [69, 70]. Necrotizing fasciitis (NF) is a severe form of fasciitis that requires urgent surgical intervention (Fig. 6d) [71]. Fascias are classified by anatomists into three locations: (1) fascia superficialis or cutaneous fascia, (2) superficial aponeurosis or deep fascia, and (3) intermuscular septa [72, 73]. In the current literature by radiologists, surgeons, and pediatric physicians, location (1) corresponds to the hypodermis, location (2) corresponds to superficial fascia, and location (3) corresponds to deep fascia [72].

Method of ultrasound

In patients with soft tissue infection, the area of interest is carefully evaluated [70]. Pediatric patients sometimes present with nonspecific clinical signs, and their parents may not reveal adequate medical history owing to abuse.

Discussion of the interpretation of the sonographic findings of soft tissue infection

Fluid accumulation in the superficial fascia or deep fascia can present as NF [68, 74, 75]. Fluid accumulation greater than 2 mm is a useful tool for diagnosing NF [74]. In cases where ultrasound evaluation is challenging, MRI could provide useful information for diagnosing NF [68, 75].

Septic arthritis and osteomyelitis

Background

Septic arthritis, also known as pyogenic arthritis, sometimes coexist with osteomyelitis (Fig. 7a–d) [76]. The metaphyseal spongiosa has a capillary loop of blood vessels, and this location is prone to initial bacterial infection due to stagnation of the bloodstream [77, 78]. In children under 18 months of age, vessel communication exists between the metaphysis, physis, and epiphysis [78, 79]. Therefore, bacteria can lodge at the metaphyseal focus and can spread into the joint through the epiphysis [78]. Another route of spread involves the bacteria lodging at the metaphyseal focus and spreading into the sub-periosteal bone through the vascularized cambium [80]. The fibrous layer of the periosteum is separated from the
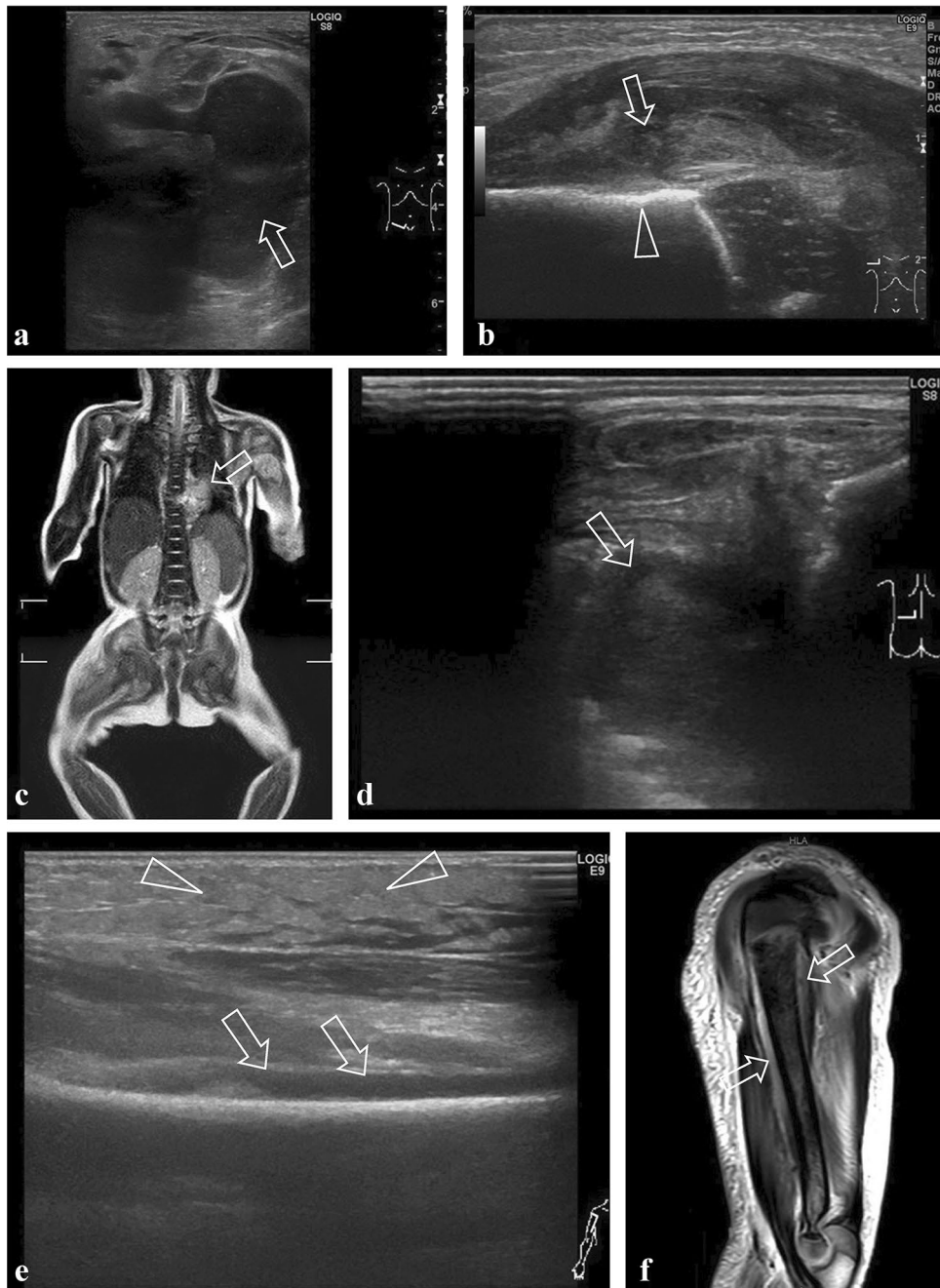
underlying parent bone by an abscess [78]. Sub-periosteal abscess is one of the accompanying complications of acute osteomyelitis, and percutaneous drainage may be recommended (Fig. 7e, f) [8, 81]. In addition, the synovium may be infected directly through bloodstream infection [82]. Surgical treatment for septic arthritis involves urgent decompression of the joint via open arthrotomy, irrigation, and debridement [2]. Furthermore, acute osteomyelitis requires an adequate period of antibiotics, and sequestrectomy is recommended if a sequestrum is present [83, 84].

Methods of ultrasound

Pediatric patients should be appropriately positioned to evaluate the area of suspected infectious disease [85]. For evaluation of the bone cortex, a longitudinal view parallel to the bone cortex is warranted to detect its destruction. During the evaluation of joint effusion, in addition to observation from the frontal view, observation from multiple directions, such as the lateral view, is warranted.

◄**Fig. 7** **a–d** Imaging findings of a one-month-old female patient with septic arthritis and discitis. She was admitted to our hospital for septic shock. Her blood pressure was 60/80 mmHg, pulse rate 210 bpm, temperature 39.9 °C, and oxygen saturation (SpO_2) was 100% with 1 L/minute oxygen via nasal cannula. Blood test results revealed a white blood cell count of 1400/mm³ and C-reactive protein of 13.4 mg/dL. Blood culture revealed methicillin-susceptible *Staphylococcus aureus*. Ultrasound of the right hip and shoulder revealed echogenic fluid collection. Proximal bone cortex of the humerus revealed destruction. Coronal whole-body magnetic resonance imaging (MRI) revealed discitis with abscess formation. Intravenous antibiotic treatment was administered for two months and subsequently switched to oral antibiotic treatment. **a** Axial sonogram of the right hip showing fluid distending the hip joint capsule (arrow). **b** Axial sonogram of the right shoulder showing echogenic fluid collection (arrow). The proximal bone cortex of the humerus shows destruction (arrowhead). **c** Coronal whole-body MRI showing discitis between thoracic vertebrae 9 and 10 (arrow). Abscess formation was also detected adjacent to the discitis. **d** Sonogram in the para-spinal approach showing low echoic fluid collection (arrow). Abscess formation resulting from discitis was diagnosed. **e**, **f** Imaging findings of a 11-month-old male patient with sub-periosteal abscess. He had a swelling in the right arm and high fever one day before. Blood test results revealed a white blood cell count of 17,500/mm³ and C-reactive protein of 17.8 mg/dL. Ultrasound revealed fluid collection around the right humerus. MRI revealed humeral osteomyelitis and sub-periosteal abscess. Methicillin-resistant *Staphylococcus aureus* was detected in the blood culture. Surgical incision, drainage, and sequential intravenous antibiotic treatment were performed for 6 weeks. Treatment was considered successful. **e** Ultrasound showing fluid collection around the right humerus (arrow). Diffuse thickening and increased echogenicity of the subcutaneous tissue are evident (arrowhead). **f** Enhanced fat-suppression T2-weighted MRI showing humeral osteomyelitis and sub-periosteal abscess (arrow)

Discussion of the interpretation of the sonographic findings of arthritis and osteomyelitis

Joint effusion can easily be revealed by ultrasound [8, 86]. If needed, another joint can be evaluated because multiple joints may be affected [2]. In addition, other locations, such as the spinal disks (discitis), may be the focus of infection [87, 88]. Sub-periosteal effusion is also detected easily by ultrasound in the affected bone [8, 81, 89]. Extension into the superficial soft tissue via the fibrous layer of the periosteum has also been detected in previous studies [8]. Disruption/erosion of the bone cortex may be difficult to evaluate using ultrasound [89]. In general, MRI is a better imaging modality than ultrasound for evaluating bone marrow edema or infarction [7].

Surgical-site infection

Background

Surgical-site infection (SSI) is divided into three groups: superficial incisional infection (SII; Fig. 8a) which includes only the skin or subcutaneous tissue; deep incisional infection (DII; Fig. 8b, c) which includes the deep soft tissue; and organ or body space infection (organ/space SSI; Fig. 8d, e) [90, 91]. Organ/space SSIs are reportedly associated with a higher mortality rate than SII and DII [92]. In SSIs after cardiovascular surgery, treatment periods and methods were changed based on previous SSI groups and the presence of sternal osteomyelitis [93–95]. In cases of organ/space SSIs, such as mediastinitis, surgical intervention is usually needed [96].

Methods of ultrasound

Scanning the area of interest after surgery would likely involve the removal of the surgical dressings. Coordination with nurses may aid in facilitating these scans and in acquiring high-quality images.

Discussion of the interpretation of the sonographic findings of for SSI

In ultrasound to evaluate the SSI, classification based on the extent of inflammation is important. In cases of SSI after cardiovascular surgery, SII or DII were detected with a higher occurrence of increased parasternal fat echogenicity, and organ/space SSI was detected as retrosternal mediastinal fluid collection [97, 98]. None of the patients without mediastinal fluid collection or increased fat echogenicity was diagnosed with organ/space SSIs [98]. Mediastinal fluid collection is an important finding in the diagnosis of organ/space SSIs on CT [99, 100]. Regarding osteomyelitis occurring at the sternum, fluid effusion between reconstructed sternal bones may be detected as osteomyelitis [97]. After cardiovascular surgery, to differentiate SSI from postsurgical changes, such as hematoma, information regarding the interval between the day of examination and surgery is useful [97]. Organ/space SSI after cardiovascular surgery usually occurs two weeks after surgery, and hematoma usually occurs within one week after surgery [98–101].

Conclusions

Ultrasound determines the extent and location of inflammation, which is important in formulating a treatment plan. The period of antibiotic treatment and need for surgical intervention are usually determined based on the physical assessment and image findings. An ultrasound could provide additional information for decision-making for the treatment of infectious diseases in pediatric patients.
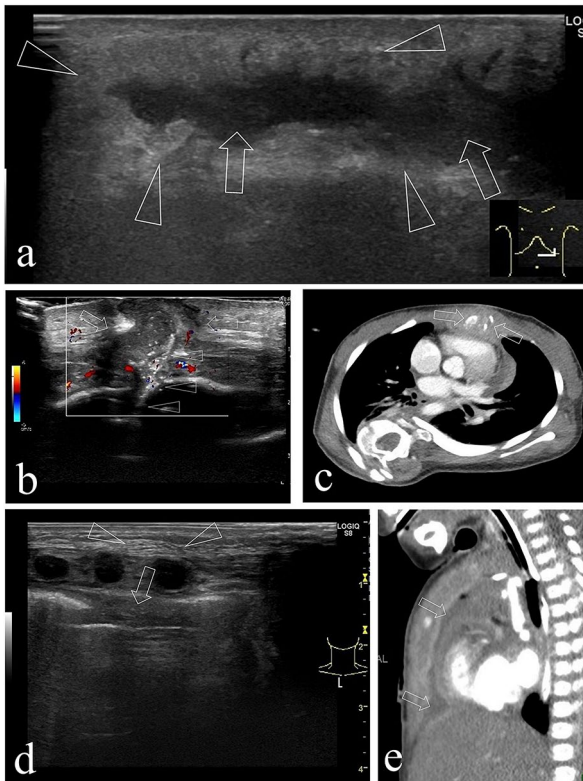
Fig. 8 a Imaging findings of a seven-year-old female patient with surgical-site infection classified as superficial incisional infection (SII). She had undergone abdominal surgery for intra-abdominal rupture of a pseudo-pancreatic cyst. She had a high fever 14 days postoperatively and a swelling at the incision site. Blood test results revealed a white blood cell count of 8560/mm^3 and C-reactive protein of 0.52 mg/dL. Ultrasound revealed fluid collection. SII with abscess formation was surgically diagnosed. *Staphylococcus epidermis* was detected in the pus. Ultrasound was performed 14 days postoperatively. Hyper-echogenicity was visualized in the region of the subcutaneous fat (arrowheads), and fluid collection (arrows) was visualized in the subcutaneous tissue. SII with abscess formation was surgically diagnosed. **b**, **c** Imaging findings of a five-year-old female patient with surgical-site infection classified as deep incisional infection (DII). She had a high fever 11 days postoperatively. Her temperature was 38.0 °C. Blood test results revealed a white blood cell count of 7100/mm^3 and C-reactive protein of 0.23 mg/dL. Ultrasound and computed tomography (CT) revealed inflammation in the region of the subcutaneous fat and around the sternum with osteolytic change. DII with osteomyelitis with sequestrum at the sternum was surgically diagnosed. Debridement was performed, and *Pseudomonas aeruginosa* was detected. **b** Ultrasound was performed 11 days postoperatively. Hyperechogenicity was visualized in the region of subcutaneous fat and around the sternum (arrow). Fluid collection (arrows) with hyperechoic foci (arrowheads) was visualized between the reconstructed sternal bodies. **c** Axial contrast-enhanced CT showing low attenuation around the sternum. Osteolytic change (arrow) was detected in the reconstructed sternum; hence, osteomyelitis was suspected. DII with osteomyelitis sequestrum at the sternum was surgically diagnosed. **d**, **e** Imaging findings of a four-month-old male patient with surgical-site infection classified as organ/space surgical-site infection. A four-month-old male patient had a high fever 10 days postoperatively. Blood test results revealed a white blood cell count of 11,160/mm^3 and C-reactive protein of 15.7 mg/dL. Ultrasound and CT revealed anterior mediastinal fluid collection and infection

extending into the organ/space, which was proven surgically. *Pseudomonas aeruginosa* was detected, and intravenous antibiotics therapy was administered for nine weeks. The treatment was considered successful. **d** Ultrasound was performed 10 days postoperatively. Anterior mediastinal fluid was detected (arrow), and hyper-echogenicity was visualized in the region of the subcutaneous fat (arrowheads). **e** Sagittal reconstructed contrast-enhanced CT showing fluid at the retrosternal space with air bubbles (arrow). Infection extending into the organ/space was proven surgically

Declarations

Ethical approval This research was performed in accordance with the tenets of the Declaration of Helsinki and was approved by the ethics committee of our institution (Ethical number: 2021-01-003).

Conflict of interest No financial or non-financial benefits have been received or will be received from any party related directly or indirectly to the subject of this article.

Consent for publication Some patients have given their informed consent on the electronic medical record and Japanese law requires to save electronic medical records, but in this review, it also includes patients who have already completed treatment and have not been followed up in our hospital. Therefore, ethinical permission was obtained from the ethics committee of our hospital.

References

1. Meissner HC. Viral bronchiolitis in children. N Engl J Med. 2016;374:62–72.
2. Montgomery NI, Epps HR. Pediatric septic arthritis. Orthop Clin North Am. 2017;48:209–16.
3. Bradley JS, Byington CL, Shah SS, Alverson B, Carter ER, Harrison C, et al. The management of community-acquired pneumonia in infants and children older than 3 months of age: clinical practice guidelines by the Pediatric Infectious Diseases Society and the Infectious Diseases Society of America. Clin Infect Dis. 2011;53:e25–76.
4. Brook I. Intra-abdominal, retroperitoneal, and visceral abscesses in children. Eur J Pediatr Surg. 2004;14:265–73.
5. Hoen LA, Bogaert G, Radmayr C, Dogan HS, Nijman RJM, Quaedackers J, et al. Update of the EAU/ESPU guidelines on urinary tract infections in children. J Pediatr Urol. 2021;17:200–7.
6. Schleifer J, Liteplo AS, Kharasch S. Point-of-care ultrasound in a child with chest wall pain and rib osteomyelitis. J Emerg Med. 2019;57:550–3.

7. Schmit P, Glorion C. Osteomyelitis in infants and children. Eur Radiol. 2004;14:L44–54.

8. Shahid M, Holton C, O'Riordan S, Kraft JK. Sonography of musculoskeletal infection in children. Ultrasound. 2020;28:103–17.

9. Toro MS, Martínez JLV, Falcão RV, Prata-Barbosa A, Cunha A. Point-of-care ultrasound by the pediatrician in the diagnosis and follow-up of community-acquired pneumonia. J Pediatr (Rio J). 2021;97:13–21.

10. Robben SG. Ultrasonography of musculoskeletal infections in children. Eur Radiol. 2004;14:L65-77.

11. Motahari SJ, Poormoosa R, Nikkhah M, Bahari M, Shirazy SM, Khavarinejad F. Treatment and prognosis of deep neck infections. Indian J Otolaryngol Head Neck Surg. 2015;67:134–7.

12. Côrte FC, Firmino-Machado J, Moura CP, Spratley J, Santos M. Acute pediatric neck infections: outcomes in a seven-year series. Int J Pediatr Otorhinolaryngol. 2017;99:128–34.

13. Hosokawa T, Tanami Y, Sato Y, Ishimaru T, Kawashima H, Oguma E. Comparison of sonographic findings between neonates with pyriform sinus fistulas and lymphangiomas. Am J Otolaryngol. 2021;42:102783.

14. Hoang JK, Branstetter BF, Eastwood JD, Glastonbury CM. Multiplanar CT and MRI of collections in the retropharyngeal space: is it an abscess? AJR Am J Roentgenol. 2011;196:W426–32.

15. Zhao X, Delaney M, Breslin K, Chamberlain JM, Rubio EI, Reilly BK, et al. Impact of transcervical ultrasound for the diagnosis of pediatric peritonsillar abscesses on emergency department performance measures. J Ultrasound Med. 2020;39:715–20.

16. Bandarkar AN, Adeyiga AO, Fordham MT, Preciado D, Reilly BK. Tonsil ultrasound: technical approach and spectrum of pediatric peritonsillar infections. Pediatr Radiol. 2016;46:1059–67.

17. Straughan AJ, Badger CD, Benito DA, Joshi AS. Salivary gland ultrasound training: improving anatomic identification in residents. Am J Otolaryngol. 2020;41:102734.

18. Hosokawa T, Yamada Y, Sato Y, Tanami Y, Amano H, Fujiogi M, et al. Five neonatal cases of pyriform sinus fistula with cervical cystic lesion: a comparison between sonography and other modalities. J Med Ultrason. 2001;2015:579–85.

19. Hosokawa T, Yamada Y, Takahashi H, Tanami Y, Sato Y, Hosokawa M, et al. Size of the tonsil on ultrasound in children without tonsil-associated symptoms. Ultrasound Q. 2020;36:24–31.

20. Cramer JD, Purkey MR, Smith SS, Schroeder JW Jr. The impact of delayed surgical drainage of deep neck abscesses in adult and pediatric populations. Laryngoscope. 2016;126:1753–60.

21. Hah YM, Jung AR, Lee YC, Eun YG. Risk factors for transcervical incision and drainage of pediatric deep neck infections. J Pediatr Surg. 2018;53:666–70.

22. Balfour-Lynn IM, Abrahamson E, Cohen G, Hartley J, King S, Parikh D, et al. BTS guidelines for the management of pleural infection in children. Thorax. 2005;60:i1–21.

23. Sundaralingam A, Banka R, Rahman NM. Management of pleural infection. Pulm Ther. 2021;7:1–16.

24. Chung JH, Lee SH, Kim KT, Jung JS, Son HS, Sun K. Optimal timing of thoracoscopic drainage and decortication for empyema. Ann Thorac Surg. 2014;97:224–9.

25. Li W, Shen M, Zhang Y, Cong Y, Zu H, Chen H, et al. A model for predicting malignant sub-pleural solid masses using grayscale ultrasound and ultrasound elastography. Ultrasound Med Biol. 2021;47:1212–8.

26. Hardie W, Bokulic R, Garcia VF, Reising SF, Christie CD. Pneumococcal pleural empyemas in children. Clin Infect Dis. 1996;22:1057–63.

27. Patel KM, Ullah K, Patail H, Ahmad S. Ultrasound for pleural disease: beyond a pocket of pleural fluid. Ann Am Thorac Soc. 2021;18:749–56.

28. Buonsenso D, Brancato F, Valentini P, Curatola A, Supino M, Musolino AM. The use of lung ultrasound to monitor the antibiotic response of community-acquired pneumonia in children: a preliminary hypothesis. J Ultrasound Med. 2020;39:817–26.

29. Stadler JAM, Andronikou S, Zar HJ. Lung ultrasound for the diagnosis of community-acquired pneumonia in children. Pediatr Radiol. 2017;47:1412–9.

30. Same RG, Amoah J, Hsu AJ, Hersh AL, Sklansky DJ, Cosgrove SE, et al. The association of antibiotic duration with successful treatment of community-acquired pneumonia in children. J Pediatr Infect Dis Soc. 2021;10:267–73.

31. Streck HL, Goldman JL, Lee BR, Sheets JM, Wirtz AL. Evaluation of the treatment of aspiration pneumonia in hospitalized children. J Pediatr Infect Dis Soc. 2022;11:102–7.

32. Masarweh K, Gur M. Factors associated with complicated pneumonia in children. Pediatr Pulmonol. 2021;56:2700–6.

33. Kanitra JJ, Thampy CA, Cullen ML. A decade's experience of pediatric lung abscess and empyema at a community hospital. Pediatr Pulmonol. 2021;56:1245–51.

34. Buonsenso D, Tomà P, Pirozzi N, Mesturino A, Morello R, Curatola A, et al. Lung ultrasound in infants with respiratory infections: more important the age or the pathogen? Ultrasound Q. 2020;36:118–22.

35. Musolino AM, Tomà P, Supino MC, Scialanga B, Mesturino A, Scateni S, et al. Lung ultrasound features of children with complicated and noncomplicated community acquired pneumonia: a prospective study. Pediatr Pulmonol. 2019;54:1479–86.

36. Cheong I. Ultrasonography in the diagnosis of lung abscess. J Clin Ultrasound. 2022;50:628–9.

37. Huyler A, Mackenzie D, Wilson CN. Lung abscess diagnosed by ultrasound. Clin Exp Emerg Med. 2022;9:70–1.

38. Kuhajda I, Zarogoulidis K, Tsirgogianni K, Tsavlis D, Kioumis I, Kosmidis C, et al. Lung abscess-etiology, diagnostic and treatment options. Ann Transl Med. 2015;3:183.

39. Supino MC, Buonsenso D, Scateni S, Scialanga B, Mesturino MA, Bock C, et al. Point-of-care lung ultrasound in infants with bronchiolitis in the pediatric emergency department: a prospective study. Eur J Pediatr. 2019;178:623–32.

40. Bueno-Campaña M, Sainz T, Alba M, Del Rosal T, Mendez-Echevarría A, Echevarria R, et al. Lung ultrasound for prediction of respiratory support in infants with acute bronchiolitis: a cohort study. Pediatr Pulmonol. 2019;54:873–80.

41. Bobillo-Perez S, Sorribes C, Gebellí P, Lledó N, Castilla M, Ramon M, et al. Lung ultrasound to predict pediatric intensive care admission in infants with bronchiolitis (LUSBRO study). Eur J Pediatr. 2021;180:2065–72.

42. Copetti R, Cattarossi L. Ultrasound diagnosis of pneumonia in children. Radiol Med. 2008;113:190–8.

43. Rodriguez-Gonzalez M, Rodriguez-Campoy P, Estalella-Mendoza A, Castellano-Martinez A, Flores-Gonzalez JC. Characterization of cardiopulmonary interactions and exploring their prognostic value in acute bronchiolitis: a prospective cardiopulmonary ultrasound study. Tomography. 2022;8:142–57.

44. American Academy of Pediatrics Subcommittee on Diagnosis and Management of Bronchiolitis. Diagnosis and management of bronchiolitis. Pediatrics. 2006;118:1774–93.

45. Krishna D, Khera D, Toteja N, Sureka B, Choudhary B, Ganakumar VM, et al. Point-of-care thoracic ultrasound in children with bronchiolitis. Indian J Pediatr. 2022. https://doi.org/10.1007/s12098-022-04117-z#citeas.

46. Basile V, Di Mauro A, Scalini E, Comes P, Lofù I, Mostert M, et al. Lung ultrasound: a useful tool in diagnosis and management of bronchiolitis. BMC Pediatr. 2015;15:63.

47. Mongodi S, De Vita N, Salve G, Bonaiti S, Daverio F, Cavagnino M, et al. The role of lung ultrasound monitoring in early detection of ventilator-associated pneumonia in covid-19

patients: a retrospective observational study. J Clin Med. 2022;11:3001.

48. Bima P, Pivetta E, Baricocchi D, Giamello JD, Risi F, Vesan M, et al. Lung ultrasound improves outcome prediction over clinical judgment in covid-19 patients evaluated in the emergency department. J Clin Med. 2022;11:3032.

49. Bitsori M, Raissaki M, Maraki S, Galanakis E. Acute focal bacterial nephritis, pyonephrosis and renal abscess in children. Pediatr Nephrol. 2015;30:1987–93.

50. Rosenfield AT, Glickman MG, Taylor KJ, Crade M, Hodson J. Acute focal bacterial nephritis (acute lobar nephronia). Radiology. 1979;132:553–61.

51. Cheng CH, Tsau YK, Lin TY. Effective duration of antimicrobial therapy for the treatment of acute lobar nephronia. Pediatrics. 2006;117:e84–9.

52. Comploj E, Cassar W, Farina A, Gasparella P, Trenti E, Palermo S, et al. Conservative management of paediatric renal abscess. J Pediatr Urol. 2013;9:1214–7.

53. Linder BJ, Granberg CF. Pediatric renal abscesses: a contemporary series. J Pediatr Urol. 2016;12:e1-5.

54. Haber HP, Seitz G, Warmann SW, Fuchs J. Transperineal sonography for determination of the type of imperforate anus. AJR Am J Roentgenol. 2007;189:1525–9.

55. Hosokawa T, Yamada Y, Tanami Y, Sato Y, Ishimaru T, Tanaka Y, et al. Comparison of diagnostic accuracy for fistulae at ultrasound and voiding cystourethrogram in neonates with anorectal malformation. Pediatr Radiol. 2019;49:609–16.

56. Hosokawa T, Tanami Y, Sato Y, Oguma E. Comparison of imaging findings between acute focal bacterial nephritis (acute lobar nephronia) and acute pyelonephritis: a preliminary evaluation of the sufficiency of ultrasound for the diagnosis of acute focal bacterial nephritis. Emerg Radiol. 2020;27:405–12.

57. Cheng CH, Tsau YK, Lin TY. Is acute lobar nephronia the midpoint in the spectrum of upper urinary tract infections between acute pyelonephritis and renal abscess? J Pediatr. 2010;156:82–6.

58. Majd M, Nussbaum Blask AR, Markle BM, Shalaby-Rana E, Pohl HG, Park JS, et al. Acute pyelonephritis: comparison of diagnosis with 99mTc-DMSA, SPECT, spiral CT, MR imaging, and power Doppler US in an experimental pig model. Radiology. 2001;218:101–8.

59. Mitterberger M, Pinggera GM, Colleselli D, Bartsch G, Strasser H, Steppan I, et al. Acute pyelonephritis: comparison of diagnosis with computed tomography and contrast-enhanced ultrasonography. BJU Int. 2008;101:341–4.

60. Solomkin JS, Mazuski JE, Bradley JS, Rodvold KA, Goldstein EJ, Baron EJ, et al. Diagnosis and management of complicated intra-abdominal infection in adults and children: guidelines by the Surgical Infection Society and the Infectious Diseases Society of America. Clin Infect Dis. 2010;50:133–64.

61. Waked B, Holvoet T, Geldof J, Baert F, Pattyn P, Lobaton T, et al. Conservative management of spontaneous intra-abdominal abscess in Crohn's: outcome and prognostic factors. J Dig Dis. 2021;22:263–70.

62. Vaos G, Dimopoulou A, Gkioka E, Zavras N. Immediate surgery or conservative treatment for complicated acute appendicitis in children? A meta-analysis. J Pediatr Surg. 2019;54:1365–71.

63. Andersson RE, Petzold MG. Nonsurgical treatment of appendiceal abscess or phlegmon: a systematic review and meta-analysis. Ann Surg. 2007;246:741–8.

64. Mazuski JE, Tessier JM, May AK, Sawyer RG, Nadler EP, Rosengart MR, et al. The surgical infection society revised guidelines on the management of intra-abdominal infection. Surg Infect (Larchmt). 2017;18:1–76.

65. Jaffe TA, Nelson RC. Image-guided percutaneous drainage: a review. Abdom Radiol (NY). 2016;41:629–36.

66. Hosokawa T, Yamada Y, Tanami Y, Sato Y, Ishimaru T, Kawashima H, et al. Associations between sonographic findings and operative time of transumbilical laparoscopic-assisted appendectomy for acute appendicitis in children. AJR Am J Roentgenol. 2019;213:191–9.

67. Hadley GP. Intra-abdominal sepsis–epidemiology, aetiology and management. Semin Pediatr Surg. 2014;23:357–62.

68. Schmid MR, Kossmann T, Duewell S. Differentiation of necrotizing fasciitis and cellulitis using MR imaging. AJR Am J Roentgenol. 1998;170:615–20.

69. Taira BR, Singer AJ, Thode HC Jr, Lee CC. National epidemiology of cutaneous abscesses: 1996 to 2005. Am J Emerg Med. 2009;27:289–92.

70. Fried J, Tsao J, Davis L. Point-of-care ultrasound used to distinguish between superficial skin abscess and deep mediastinal abscess: a case report. J Emerg Med. 2021;60:e23–5.

71. Gafur OA, Copley LA, Hollmig ST, Browne RH, Thornton LA, Crawford SE. The impact of the current epidemiology of pediatric musculoskeletal infection on evaluation and treatment guidelines. J Pediatr Orthop. 2008;28:777–85.

72. Malghem J, Lecouvet FE, Omoumi P, Maldague BE, Vande Berg BC. Necrotizing fasciitis: contribution and limitations of diagnostic imaging. Joint Bone Spine. 2013;80:146–54.

73. Levenson RB, Singh AK, Novelline RA. Fournier gangrene: role of imaging. Radiographics. 2008;28:519–28.

74. Lin CN, Hsiao CT, Chang CP, Huang TY, Hsiao KY, Chen YC, et al. The relationship between fluid accumulation in ultrasonography and the diagnosis and prognosis of patients with necrotizing fasciitis. Ultrasound Med Biol. 2019;45:1545–50.

75. Chaudhry AA, Baker KS, Gould ES, Gupta R. Necrotizing fasciitis and its mimics: what radiologists need to know. AJR Am J Roentgenol. 2015;204:128–39.

76. Manz N, Krieg AH, Heininger U, Ritz N. Evaluation of the current use of imaging modalities and pathogen detection in children with acute osteomyelitis and septic arthritis. Eur J Pediatr. 2018;177:1071–80.

77. Travers V, Koechlin P, Apoil A, Bonnet JC. Treatment of acute pyogenic arthritis of major joints of the limbs. Rev Chir Orthop Repar Appar Mot. 1985;71:235–40 **(in French)**.

78. Jaramillo D, Dormans JP, Delgado J, Laor T, St Geme JW. Hematogenous osteomyelitis in infants and children: imaging of a changing disease. Radiology. 2017;283:629–43.

79. Stephen RF, Benson MK, Nade S. Misconceptions about childhood acute osteomyelitis. J Child Orthop. 2012;6:353–6.

80. Unkila-Kallio L, Kallio MJ, Peltola H. Acute haematogenous osteomyelitis in children in Finland. Finnish Study Group. Ann Med. 1993;25:545–9.

81. Hoffer FA, Emans J. Percutaneous drainage of subperiosteal abscess: a potential treatment for osteomyelitis. Pediatr Radiol. 1996;26:879–81.

82. Truong J, Mabrouk A, Ashurst JV. Septic bursitis. In: StatPearls. Treasure Island: StatPearls; 2022.

83. Peltola H, Pääkkönen M, Kallio P, Kallio MJ. Prospective, randomized trial of 10 days versus 30 days of antimicrobial treatment, including a short-term course of parenteral therapy, for childhood septic arthritis. Clin Infect Dis. 2009;48:1201–10.

84. Peltola H, Pääkkönen M, Kallio P, Kallio MJ. Short- versus long-term antimicrobial treatment for acute hematogenous osteomyelitis of childhood: prospective, randomized trial on 131 culture-positive cases. Pediatr Infect Dis J. 2010;29:1123–8.

85. Kim HHR, Ngo AV, Maloney E, Otjen JP, Iyer RS, Menashe SJ, et al. Contemporary imaging of the pediatric shoulder: pearls and pitfalls. Pediatr Radiol. 2021;51:338–52.

86. Kim DK, Lee JW, Na YS, Kim MJ, Lee JH, Park CH. Clinical factor for successful nonsurgical treatment of pediatric peritonsillar abscess. Laryngoscope. 2015;125:2608–11.

87. Fernandez M, Carrol CL, Baker CJ. Discitis and vertebral osteomyelitis in children: an 18-year review. Pediatrics. 2000;105:1299–304.

88. Ernat J, Riccio AI, Fitzpatrick K, Jo C, Wimberly RL. Osteomyelitis is commonly associated with septic arthritis of the shoulder in children. J Pediatr Orthop. 2017;37:547–52.

89. Riebel TW, Nasir R, Nazarenko O. The value of sonography in the detection of osteomyelitis. Pediatr Radiol. 1996;26:291–7.

90. Horan TC, Gaynes RP, Martone WJ, Jarvis WR, Emori TG. CDC definitions of nosocomial surgical site infections, 1992: a modification of CDC definitions of surgical wound infections. Infect Control Hosp Epidemiol. 1992;13:606–8.

91. Chopra T, Zhao JJ, Alangaden G, Wood MH, Kaye KS. Preventing surgical site infections after bariatric surgery: value of perioperative antibiotic regimens. Expert Rev Pharmacoecon Outcomes Res. 2010;10:317–28.

92. Poulsen KB, Bremmelgaard A, Sørensen AI, Raahave D, Petersen JV. Estimated costs of postoperative wound infections: a case-control study of marginal hospital and social security costs. Epidemiol Infect. 1994;113:283–95.

93. Yamashiro T, Kamiya H, Murayama S, Unten S, Nakayama T, Gibo M, et al. Infectious mediastinitis after cardiovascular surgery: role of computed tomography. Radiat Med. 2008;26:343–7.

94. Yamaguchi H, Yamauchi H, Yamada T, Ariyoshi T, Aikawa H, Kato Y. Diagnostic validity of computed tomography for mediastinitis after cardiac surgery. Ann Thorac Cardiovasc Surg. 2001;7:94–8.

95. Tortoriello TA, Friedman JD, McKenzie ED, Fraser CD, Feltes TF, Randall J, et al. Mediastinitis after pediatric cardiac surgery: a 15-year experience at a single institution. Ann Thorac Surg. 2003;76:1655–60.

96. Phoon PHY, Hwang NC. Deep sternal wound infection: diagnosis, treatment and prevention. J Cardiothorac Vasc Anesth. 2020;34:1602–13.

97. Hosokawa T, Suzuki S, Tanami Y, Sato Y, Ko Y, Nomura K, et al. Ultrasound evaluation of complications after cardiovascular surgery in pediatric patients: a case series. Med Ultrason. 2020;22:110–5.

98. Hosokawa T, Tanami Y, Sato Y, Ko Y, Nomura K, Oguma E. Comparison of sonographic findings between pediatric patients with mediastinitis and without mediastinitis after cardiovascular surgery. J Med Ultrason. 2001;2020:625–33.

99. Hosokawa T, Yamada Y, Tanami Y, Sato Y, Ko Y, Nomura K, et al. Computed tomography findings of mediastinitis after cardiovascular surgery. Pediatr Int. 2020;62:206–13.

100. Foldyna B, Mueller M, Etz CD, Luecke C, Haunschild J, Hoffmann I, et al. Computed tomography improves the differentiation of infectious mediastinitis from normal postoperative changes after sternotomy in cardiac surgery. Eur Radiol. 2019;29:2949–57.

101. Abu-Omar Y, Kocher GJ, Bosco P, Barbero C, Waller D, Gudbjartsson T, et al. European Association for Cardio-Thoracic Surgery expert consensus statement on the prevention and management of mediastinitis. Eur J Cardiothorac Surg. 2017;51:10–29.